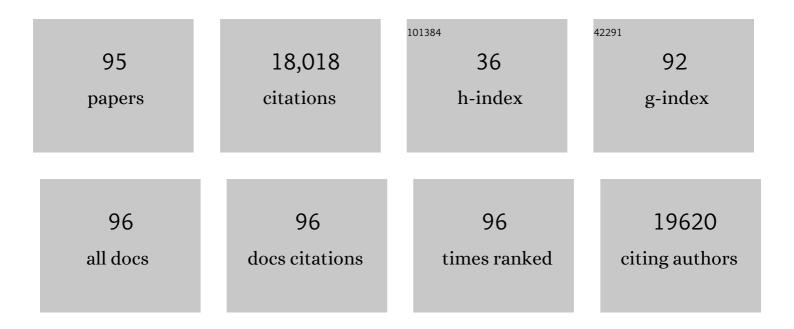
Katsumi Kaneko

List of Publications by Year in descending order

Source: https://exaly.com/author-pdf/3534270/publications.pdf Version: 2024-02-01



#	Article	IF	CITATIONS
1	Physisorption of gases, with special reference to the evaluation of surface area and pore size distribution (IUPAC Technical Report). Pure and Applied Chemistry, 2015, 87, 1051-1069.	0.9	12,159
2	Mesopore-Modified Zeolites:Â Preparation, Characterization, and Applications. Chemical Reviews, 2006, 106, 896-910.	23.0	1,016
3	Determination of pore size and pore size distribution. Journal of Membrane Science, 1994, 96, 59-89.	4.1	581
4	Simulation study on the relationship between a high resolution αs-plot and the pore size distribution for activated carbon. Carbon, 1998, 36, 1459-1467.	5.4	251
5	Conducting linear chains of sulphur inside carbon nanotubes. Nature Communications, 2013, 4, 2162.	5.8	228
6	Partial breaking of the Coulombic ordering of ionic liquids confined in carbon nanopores. Nature Materials, 2017, 16, 1225-1232.	13.3	219
7	Nitrogen Adsorption in Slit Pores at Ambient Temperatures: Comparison of Simulation and Experiment. Langmuir, 1994, 10, 4606-4609.	1.6	211
8	Quantum Effects on Hydrogen Isotope Adsorption on Single-Wall Carbon Nanohorns. Journal of the American Chemical Society, 2005, 127, 7511-7516.	6.6	189
9	Freezing of simple fluids in microporous activated carbon fibers: Comparison of simulation and experiment. Journal of Chemical Physics, 1999, 111, 9058-9067.	1.2	164
10	Uniform Mesopore-Donated Zeolite Y Using Carbon Aerogel Templating. Journal of Physical Chemistry B, 2003, 107, 10974-10976.	1.2	148
11	A new determination method of absolute adsorption isotherm of supercritical gases under high pressure with a special relevance to density-functional theory study. Journal of Chemical Physics, 2001, 114, 4196-4205.	1.2	130
12	Intrapore fieldâ€dependent micropore filling of supercritical N2 in slitâ€shaped micropores. Journal of Chemical Physics, 1992, 97, 8705-8711.	1.2	125
13	Micropore Size Distribution of Activated Carbon Fiber Using the Density Functional Theory and Other Methods. Langmuir, 2000, 16, 4300-4304.	1.6	123
14	Effect of Purification on Pore Structure of HiPco Single-Walled Carbon Nanotube Aggregates. Nano Letters, 2002, 2, 385-388.	4.5	107
15	Adsorption Properties of Templated Mesoporous Carbon (CMK-1) for Nitrogen and Supercritical MethaneExperiment and GCMC Simulation. Journal of Physical Chemistry B, 2002, 106, 6523-6528.	1.2	107
16	Direct Evidence on Câ^'C Single Bonding in Single-Wall Carbon Nanohorn Aggregates. Journal of Physical Chemistry C, 2007, 111, 5572-5575.	1.5	104
17	Storage of Hydrogen at 303 K in Graphite Slitlike Pores from Grand Canonical Monte Carlo Simulation. Journal of Physical Chemistry B, 2005, 109, 17174-17183.	1.2	101
18	A Remarkable Elevation of Freezing Temperature of CCl4 in Graphitic Micropores. Journal of Physical Chemistry B, 1999, 103, 7061-7063.	1.2	87

ΚΑΤSUMI ΚΑΝΕΚΟ

#	Article	IF	CITATIONS
19	Confinement in Carbon Nanospace-Induced Production of KI Nanocrystals of High-Pressure Phase. Journal of the American Chemical Society, 2011, 133, 10344-10347.	6.6	86
20	Large Area Films of Alternating Graphene–Carbon Nanotube Layers Processed in Water. ACS Nano, 2013, 7, 10788-10798.	7.3	85
21	Activation routes for high surface area graphene monoliths from graphene oxide colloids. Carbon, 2014, 76, 220-231.	5.4	85
22	Grand Canonical Monte Carlo Simulation Study of Methane Adsorption at an Open Graphite Surface and in Slitlike Carbon Pores at 273 K. Langmuir, 2005, 21, 5639-5646.	1.6	83
23	Nanowindow-Induced Molecular Sieving Effect in a Single-Wall Carbon Nanohorn. Journal of Physical Chemistry B, 2002, 106, 12668-12669.	1.2	79
24	Effect of Catalyst Size on Hydrogen Storage Capacity of Pt-Impregnated Active Carbon via Spillover. Journal of Physical Chemistry Letters, 2010, 1, 1060-1063.	2.1	78
25	Controlled Opening of Single-Wall Carbon Nanohorns by Heat Treatment in Carbon Dioxide. Journal of Physical Chemistry B, 2003, 107, 4479-4484.	1.2	74
26	Enhancement of the methylene blue adsorption rate for ultramicroporous carbon fiber by addition of mesopores. Carbon, 2006, 44, 1884-1890.	5.4	71
27	Air separation with graphene mediated by nanowindow-rim concerted motion. Nature Communications, 2018, 9, 1812.	5.8	67
28	Dynamic Quantum Molecular Sieving Separation of D ₂ from H ₂ –D ₂ Mixture with Nanoporous Materials. Journal of the American Chemical Society, 2012, 134, 18483-18486.	6.6	64
29	Prediction of Hysteresis Disappearance in the Adsorption Isotherm of N2on Regular Mesoporous Silica. Langmuir, 1998, 14, 3079-3081.	1.6	63
30	Structural prediction of graphitization and porosity in carbide-derived carbons. Carbon, 2017, 119, 1-9.	5.4	62
31	Nanostructured carbon materials for enhanced nitrobenzene adsorption: Physical vs. chemical surface properties. Carbon, 2018, 139, 833-844.	5.4	55
32	Efficient H2Adsorption by Nanopores of High-Purity Double-Walled Carbon Nanotubes. Journal of the American Chemical Society, 2006, 128, 12636-12637.	6.6	50
33	Surface Fractal Dimension of Less-Crystalline Carbon Micropore Walls. Journal of Physical Chemistry B, 1997, 101, 1845-1850.	1.2	46
34	Microporosity Development of Single-Wall Carbon Nanohorn with Chemically Induced Coalescence of the Assembly Structure. Journal of Physical Chemistry B, 2004, 108, 17775-17782.	1.2	39
35	Ambient Temperature Reduction of NO to N2 in Ru-Tailored Carbon Subnanospace. Journal of Physical Chemistry B, 1997, 101, 1938-1939.	1.2	38
36	Quantum Effects on Hydrogen Isotopes Adsorption inÂNanopores. Journal of Low Temperature Physics, 2009, 157, 352-373.	0.6	38

3

Катѕимі Калеко

#	Article	IF	CITATIONS
37	A water-resilient carbon nanotube based strain sensor for monitoring structural integrity. Journal of Materials Chemistry A, 2019, 7, 19996-20005.	5.2	36
38	Developments and structures of mesopores in alkaline-treated ZSM-5 zeolites. Adsorption, 2006, 12, 309-316.	1.4	34
39	Correlation in structure and properties of highly-porous graphene monoliths studied with a thermal treatment method. Carbon, 2016, 96, 174-183.	5.4	34
40	Super-sieving effect in phenol adsorption from aqueous solutions on nanoporous carbon beads. Carbon, 2018, 135, 12-20.	5.4	34
41	Anomaly of CH ₄ Molecular Assembly Confined in Single-Wall Carbon Nanohorn Spaces. Journal of the American Chemical Society, 2011, 133, 2022-2024.	6.6	33
42	Direct Thermal Fluorination of Single Wall Carbon Nanohorns. Journal of Physical Chemistry B, 2004, 108, 9614-9618.	1.2	32
43	Charge-transfer mediated nanopore-controlled pyrene derivatives/graphene colloids. Carbon, 2018, 139, 512-521.	5.4	31
44	Comparative pore structure analysis of highly porous graphene monoliths treated at different temperatures with adsorption of N2 at 77.4ÅK and of Ar at 87.3ÅK and 77.4ÅK. Microporous and Mesoporous Materials, 2015, 209, 72-78.	2.2	30
45	Water Adsorption Property of Hierarchically Nanoporous Detonation Nanodiamonds. Langmuir, 2017, 33, 11180-11188.	1.6	28
46	Preformed monolayer-induced filling of molecules in micropores. Chemical Physics Letters, 2000, 326, 158-162.	1.2	27
47	The structural change of graphitization-controlled microporous carbon upon adsorption of H2O and N2. Chemical Physics Letters, 1992, 191, 569-573.	1.2	24
48	Chemically and mechanically robust SWCNT based strain sensor with monotonous piezoresistive response for infrastructure monitoring. Chemical Engineering Journal, 2020, 388, 124174.	6.6	24
49	Structural Characterization of Heat-Treated Activated Carbon Fibers. Journal of Porous Materials, 1997, 4, 181-186.	1.3	22
50	Structural mechanism of reactivation with steam of pitch-based activated carbon fibers. Journal of Colloid and Interface Science, 2020, 578, 422-430.	5.0	22
51	Carbon Molecular Sieves: Reconstruction of Atomistic Structural Models with Experimental Constraints. Journal of Physical Chemistry C, 2014, 118, 12996-13007.	1.5	21
52	Ultrapermeable 2D-channeled graphene-wrapped zeolite molecular sieving membranes for hydrogen separation. Science Advances, 2022, 8, eabl3521.	4.7	21
53	Adsorption of water vapor on mesoporosity-controlled singe wall carbon nanohorn. Colloids and Interface Science Communications, 2015, 5, 8-11.	2.0	20
54	Water-selective adsorption sites on detonation nanodiamonds. Carbon, 2018, 139, 853-860.	5.4	20

ΚΑΤSUMI ΚΑΝΕΚΟ

#	Article	IF	CITATIONS
55	Sol–gel chemistry mediated Zn/Al-based complex dispersant for SWCNT in water without foam formation. Carbon, 2015, 94, 518-523.	5.4	18
56	Adsorption separation of heavier isotope gases in subnanometer carbon pores. Nature Communications, 2021, 12, 546.	5.8	18
57	Chemisorption and Photoadsorption of NO on Cerium(IV) Oxide. Langmuir, 1997, 13, 5894-5899.	1.6	16
58	High capacitance carbon-based xerogel film produced without critical drying. Applied Physics Letters, 2008, 93, 193112.	1.5	16
59	Structural adsorption mechanism of chloroform in narrow micropores of pitch-based activated carbon fibres. Carbon, 2021, 171, 681-688.	5.4	16
60	The subtracting pore effect method for an accurate and reliable surface area determination of porous carbons. Carbon, 2021, 175, 77-86.	5.4	15
61	The growth of FeOOH microcrystals and chemisorption rate of NO. Journal of Chemical Technology and Biotechnology, 1987, 37, 11-19.	1.6	14
62	Enhanced CO ₂ Adsorptivity of Partially Charged Single Walled Carbon Nanotubes by Methylene Blue Encapsulation. Journal of Physical Chemistry C, 2012, 116, 11216-11222.	1.5	14
63	Molecular States of O2 Confined in a Carbon Nanospace from the Low-Temperature Magnetic Susceptibility. Langmuir, 1997, 13, 1047-1053.	1.6	13
64	Characterization of hydrated silicate glass microballoons. Journal of Materials Research, 1996, 11, 2908-2915.	1.2	12
65	Unusual hygroscopic nature of nanodiamonds in comparison with well-known porous materials. Journal of Colloid and Interface Science, 2019, 549, 133-139.	5.0	12
66	Evaluation of Micropore Width of Activated Carbon Fibers by MultiStage Micropore Filling Analysis. Tanso, 1989, 1989, 288-295.	0.1	12
67	Iron oxide films of a spinel structure from thermal decomposition of metal ion citrate complex. Journal of Materials Research, 1999, 14, 2002-2006.	1.2	11
68	The Semiconductive Property of Gammaâ€Ferric Oxyhydroxide. Journal of the Electrochemical Society, 1975, 122, 451-452.	1.3	10
69	Formation of COx-Free H2 and Cup-Stacked Carbon Nanotubes over Nano-Ni Dispersed Single Wall Carbon Nanohorns. Langmuir, 2012, 28, 7564-7571.	1.6	10
70	Cu-phthalocyanine-mediated nanowindow production on single-wall carbon nanohorn. Molecular Physics, 2021, 119, .	0.8	10
71	Nanoporosity Change on Elastic Relaxation of Partially Folded Graphene Monoliths. Langmuir, 2017, 33, 14565-14570.	1.6	9
72	Ferromagnetic Iron Oxides from Synthetic β â€â€‰FeOOH by Vacuum Thermal Decomposition. Journal of t Electrochemical Society, 1984, 131, 2435-2438.	he 1.3	8

5

ΚΑΤSUMI ΚΑΝΕΚΟ

#	Article	IF	CITATIONS
73	Controlled growth of one-dimensional clusters of molybdenum atoms using double-walled carbon nanotube templating. Applied Physics Letters, 2009, 94, .	1.5	8
74	Reconstructing the fractal clusters of detonation nanodiamonds from small-angle X-ray scattering. Carbon, 2020, 169, 349-356.	5.4	8
75	Zn/Al complex-SWCNT ink for transparent and conducting homogeneous films by scalable bar coating method. Chemical Physics Letters, 2016, 650, 113-118.	1.2	7
76	Electrical conductivity changes of water-adsorbed nanodiamonds with thermal treatment. Chemical Physics Letters: X, 2019, 737, 100018.	2.1	7
77	Novel Structure of Microporous Activated Carbon Fibers and Their Gas Adsorption. Materials Research Society Symposia Proceedings, 1994, 349, 73.	0.1	5
78	Transition metal oxide films. Advanced Materials, 1995, 7, 312-315.	11.1	5
79	Gas storage in soft 1D nano-tunnels by the induced fit of a serration structure. CrystEngComm, 2009, 11, 347-350.	1.3	5
80	Toward in silico modeling of palladium–hydrogen–carbon nanohorn nanocomposites. Physical Chemistry Chemical Physics, 2014, 16, 11763-11769.	1.3	5
81	Mild oxidation-production of subnanometer-sized nanowindows of single wall carbon nanohorn. Journal of Colloid and Interface Science, 2018, 529, 332-336.	5.0	5
82	Mesoscopic cage-like structured single-wall carbon nanotube cryogels. Microporous and Mesoporous Materials, 2020, 293, 109814.	2.2	5
83	Highly oxidation-resistant graphene-based porous carbon as a metal catalyst support. Carbon Trends, 2021, 3, 100029.	1.4	4
84	Fundamentals of Gas Adsorption for Characterization of Carbon Materials. Tanso, 1999, 1999, 50-53.	0.1	3
85	Electric field assisted ion adsorption with nanoporous SWCNT electrodes. Adsorption, 2019, 25, 1035-1041.	1.4	2
86	A Molecular Simulation Study on Empirical Determination Method of Pore Structures of Activated Carbons. Tanso, 1997, 1997, 159-166.	0.1	2
87	Anomalous Magnetism of Activated Carbon Having Ultra High Surface Area. Tanso, 2000, 2000, 218-222.	0.1	2
88	Activated Carbon Fibres of Different Cross-Sectional Morphologies. Adsorption Science and Technology, 2004, 22, 517-522.	1.5	1
89	Phenol Molecular Sheets Woven by Water Cavities in Hydrophobic Slit Nanospaces. Langmuir, 2018, 34, 15150-15159.	1.6	1
90	Nanopore structure analysis of single wall carbon nanotube xerogels and cryogels. Adsorption, 2021, 27, 673-681.	1.4	1

Катѕимі Калеко

#	Article	IF	CITATIONS
91	Structures and Properties of Atoms and Molecules Confined in Nanospaces. Structures and Properties of Atoms and Molecules Confined in Nanoporous Spaces Hyomen Kagaku, 2000, 21, 2-9.	0.0	1
92	Pore-Mouth Structure of Highly Agglomerated Detonation Nanodiamonds. Nanomaterials, 2021, 11, 2772.	1.9	1
93	Real solid surfaces and fractal Hyomen Kagaku, 1991, 12, 34-38.	0.0	0
94	Unearthing of a new science from nanostructured carbons. Tanso, 2021, 2021, 145-160.	0.1	0
95	Apatite–Graphene Interface Channel-Aided Rapid and Selective H ₂ Permeation. Journal of Physical Chemistry C, 2022, 126, 3653-3660.	1.5	0